Grape seed proanthocyanidins induce apoptosis through the mitochondrial pathway in nasopharyngeal carcinoma CNE-2 cells

KAI YAO[1*], JINGJING SHAO[2*], KEYUAN ZHOU[2], HAITAO QIU[1], FENGXIANG CAO[1], CAIHONG LI[2] and DE DAI[1]

[1]Department of Otolaryngology of The Affiliated Hospital of Guangdong Medical University, Zhanjiang, Guangdong 524023; [2]Institute of Biochemistry and Molecular Biology, Guangdong Provincial Key Laboratory of Medical Molecular Diagnostics, Guangdong Medical University, Dongguan 523808, P.R. China

Received January 22, 2016; Accepted March 4, 2016

DOI: 10.3892/or.2016.4855

Abstract. Although modern radiotherapy offers excellent local control in the treatment of nasopharyngeal carcinoma (NPC), current therapeutic decisions remain burdensome due to the frequency of local recurrence and treatment failure at distant sites. One potential and promising strategy for the prevention or treatment of cancers is the use of bioactive components of plant origin, including dietary plant products. Herein, we studied one class of these bioactive compounds, grape seed proanthocyanidins (GSPs), and explored their effect on NPC CNE-2 cells, as well as the primary mechanism underlying this effect. Our results revealed that treatment of human NPC CNE-2 cells with GSPs reduced cell viability in a dose- and time-dependent manner, and moreover, markedly induced cell cycle arrest at the G2/M phase, leading to induction of apoptosis. In addition, we found that the underlying mechanism was associated with increased expression of the pro-apoptotic protein Bax, decreased expression of the anti-apoptotic proteins Bcl-2 and Bcl-xL, upregulation of cleaved caspase-3 and cleaved poly(ADP-ribose) polymerase (PRAP) protein, and the loss of mitochondrial membrane potential (MMP) ($\Delta\psi m$). Furthermore, GSPs upregulated the Bcl-2 homology 3 (BH3)-only proteins, Bim and Bad, in a concentration-dependent manner. Taken together, these data supported our hypothesis that, in human NPC CNE-2 cells, GSPs could induce apoptosis through the mitochondrial pathway and ultimately reduce cell viability. Collectively, the results discussed above provide substantive evidence for the potential of GSPs as an effective bioactive phytochemical for the treatment of NPC.

Correspondence to: Dr Caihong Li, Institute of Biochemistry and Molecular Biology, Guangdong Medical University, 2 Civilization Eastern Road, Xiashan, Zhanjiang, Guangdong 524023, P.R. China
E-mail: smile_lee2013@163.com

Professor De Dai, Department of Otolaryngology of The Affiliated Hospital of Guangdong Medical University, 2 Civilization Eastern Road, Xiashan, Zhanjiang, Guangdong 524023, P.R. China
E-mail: dedai@126.com

*Contributed equally

Key words: grape seed proanthocyanidins, mitochondrial pathway, nasopharyngeal carcinoma, apoptosis, Bcl-2

Introduction

Nasopharyngeal carcinoma (NPC) is a malignancy arising from the epithelium of the nasopharynx, the epicenter of which is frequently observed at the pharyngeal recess, from where the tumor invades adjacent anatomical spaces or organs (1). NPC is highly endemic in the regions of Southeast Asia, Northern Africa and the Middle East. Radiotherapy, the standard treatment for NPC, is effective in controlling early tumors with a good prognosis (2); however, treatment success largely depends on tumor stage, which, at the point of diagnosis, has often reached advanced disease. Although modern practice involves the strategy of combining chemotherapy with radiotherapy and intensity-modulated radiotherapy (IMRT), retrospective prognosis reports of patients treated with these therapeutic schemes have revealed that ~5-15% of NPC patients still have local recurrence, and 15-30% may experience failure at distant sites (3-5). Another challenge confounding treatment options is that surviving NPC patients frequently suffer late adverse events that greatly affect their quality of life, including cervical subcutaneous fibrosis, hearing loss, skin dystrophy, xerostomia and radiation-induced sarcoma of the head and neck (RISHN) (6,7). Therefore, it is of great clinical value to explore and develop more effective and less toxic therapeutic agents for the treatment of NPC.

In normal physiology, cells that have been improperly stimulated for survival are eliminating by apoptosis, a protective mechanism against neoplastic development that can be mediated by several different pathways (8). The most commonly modulated type of cell death in cancers is the mitochondrial pathway of apoptosis, also called the intrinsic pathway (9). This pathway is strictly controlled by proteins of the Bcl-2 family which induce mitochondrial outer membrane permeabilization (MOMP) (10), and are subdivided into the anti-apoptotic proteins (Bcl-2 and Bcl-xL), the pro-apoptotic proteins (Bax and Bak), and the BH3-only proteins (Bim,

Bad and Puma). Anti-apoptotic Bcl-2 proteins promote cell proliferation, while oligomerization of Bak and Bax proteins are the two primary activators of MOMP (8). An increase in the Bax/Bcl-2 ratio is critical for apoptosis and can enhance the membrane permeability of mitochondria (11). The mitochondrial apoptosis pathway provides an effective means of inducing cell death, and many drugs and macromolecules intended for cancer therapy have been targeted to this pathway.

Previous epidemiological studies have indicated that intake of fruits and vegetables may be associated with a reduced risk for various types of cancers (12). The active ingredients of grape seed extract (GSE) are grape seed proanthocyanidins (GSPs), which occur in dimers, trimers, tetramers and oligomers/polymers of monomeric catechins and/or (-)-epicatechins, and are responsible for the various aesthetic and taste-related qualities of red wine (13). GSE is commonly consumed as a dietary supplement, and is sold in the form of capsules or tablets (100-500 mg) as an over-the-counter product in the US. It has been demonstrated that GSPs have anticancer properties *in vitro* or *in vivo* in various types of cancers such as pancreatic (14), colorectal (15), cervical (16) and lung cancer (17). Furthermore, both toxicity testing in rats, as well as genotoxicity testing, have shown that GSPs have low toxicity and no genotoxic potential (18). Nevertheless, the antitumor potential of GSPs in NPC has rarely been reported.

In the present study, we aimed to investigate the chemotherapeutic potential of GSPs by examining their effect on the human-derived NPC CNE-2 cell line. Based on the reported antitumor effect, we sought to obtain a deeper understanding of the ability of GSPs to treat NPC, and elucidate the specific mechanism by which it does so, with the ultimate aim of providing a useful reference for clinical medication.

Materials and methods

Materials. Primary antibodies were obtained from the following vendors: antibodies specific for Bax, Bcl-2, Bcl-xL, Bim, Bad, pro-caspase-3, cleaved caspase-3, PARP, cleaved PARP and β-actin were purchased from Cell Signaling Technology, Inc. (Danvers, MA, USA); the horseradish peroxidase (HRP)-conjugated goat anti-rabbit IgG secondary antibodies were purchased from Bio-Rad (Hercules, CA, USA). The Annexin V-FITC/propidium iodide (PI) apoptosis detection and cell cycle assay kits were purchased from Vazyme Biotech, Inc. (Nanjing, Jiangsu, China). The JC-1 mitochondrial membrane potential (MMP) detection kit, Cell Counting Kit-8 (CCK-8), Hoechst 33258 staining kit, and all other chemicals were purchased from Beyotime Institute of Biotechnology (Haimen, Jiangsu, China). The GSPs used in the present study were purchased from Jingke Chemical, Inc. (Shanghai, China) (lot no. MUST-14081604; purity, 95%).

Cell culture. The CNE-2 human NPC cell line was obtained from the Institute of Biochemistry and Molecular Biology, Guangdong Medical University (Guangdong, China). The cells were cultured in RPMI-1640 medium (Gibco-BRL, Carlsbad, CA, USA) supplemented with 10% (v/v) fetal bovine serum (Sijiqing, Hangzhou, Zhejiang, China), 100 U/ml penicillin and 100 μg/ml streptomycin (Beyotime Institute of Biotechnology). Cells were maintained in an incubator with a humidified atmosphere of 5% CO_2 at 37˚C, subcultured and allowed to reach 70-80% confluency, before beginning experimentation.

Cell proliferation and colony formation assays. Cell proliferation was evaluated using the CCK-8 and colony formation assays. CNE-2 cells were seeded in 96-well plates at a density of 5,000 cells/well, and incubated for 24 h. The cells were then treated with 5, 10, 20, 40 and 60 μg/ml GSPs or control for 6, 12 and 24 h. At the end of the stipulated time, CCK-8 was added to each well according to the manufacturer's instructions, and the absorbance was recorded at 450 nm using a microplate reader (Bio-Rad). The effect of GSPs on cell viability was calculated in terms of the percent of the control, arbitrarily assigned as having 100% viability. All tests were carried out in triplicate, and IC_{50} values were analyzed using GraphPad Prism 5.0. For the colony formation assays, CNE-2 cells were seeded at 500 cells/well on 6-well plates and treated with 1.25, 2.5 and 5 μg/ml GSPs or control, followed by culture for 10 days in an incubator with a humidified atmosphere of 5% CO_2 at 37˚C. Visible colonies gradually emerged, and after the 10-day culture period, were stained with crystal violet and counted under a dissection microscope.

Cell cycle analysis. CNE-2 cells were treated with different concentrations of GSPs (0, 10, 20 and 40 μg/ml, the same below) for 12 h, collected, and then fixed with 75% cold ethanol overnight at -20˚C. Next, the cells were washed twice with cold phosphate-buffered saline (PBS), incubated with RNase in a 37˚C water bath for 30 min, and finally incubated with PI on ice, in the dark, as described in the Cell Cycle Assay kit (Vazyme Biotech Co., Ltd.) instructions. Cell cycle distribution was then analyzed with a FACSCanto II flow cytometer (BD Biosciences, San Jose, CA, USA) equipped with CellQuest software.

Fluorescence microscopy. Apoptotic nuclear morphology was assessed by staining the cells with the fluorescent DNA-binding dye Hoechst 33258. After a 12-h treatment with GSPs, CNE-2 cells were fixed and washed twice with PBS, and then stained with Hoechst 33258 for 30 min in the dark at room temperature. Following two washes with PBS, the nuclear morphology was observed under a fluorescence microscope (Nikon Corp., Tokyo, Japan).

Flow cytometric detection of apoptosis. GSP-induced apoptosis was also analyzed by flow cytometry, utilizing the Annexin V-FITC apoptosis detection kit (Vazyme Biotech Co., Ltd.) in accordance with the manufacturer's protocol. Briefly, CNE-2 cells were seeded in 6 cm-well plates at a density of $2x10^5$ cells, and cultured for 24 h, at which point they were treated with GSPs for 12 h. Following treatment, the cells were harvested, washed twice with cold PBS, and incubated with Annexin V-FITC and PI for 10 min in the dark. The stained cells were analyzed on a FACSCanto II flow cytometer equipped with CellQuest software. Experiments were repeated in triplicate.

Assay for MMP. The MMP of CNE-2 cells was determined using a MMP assay kit with JC-1 (Beyotime Institute of Biotechnology), according to the manufacturer's instructions.

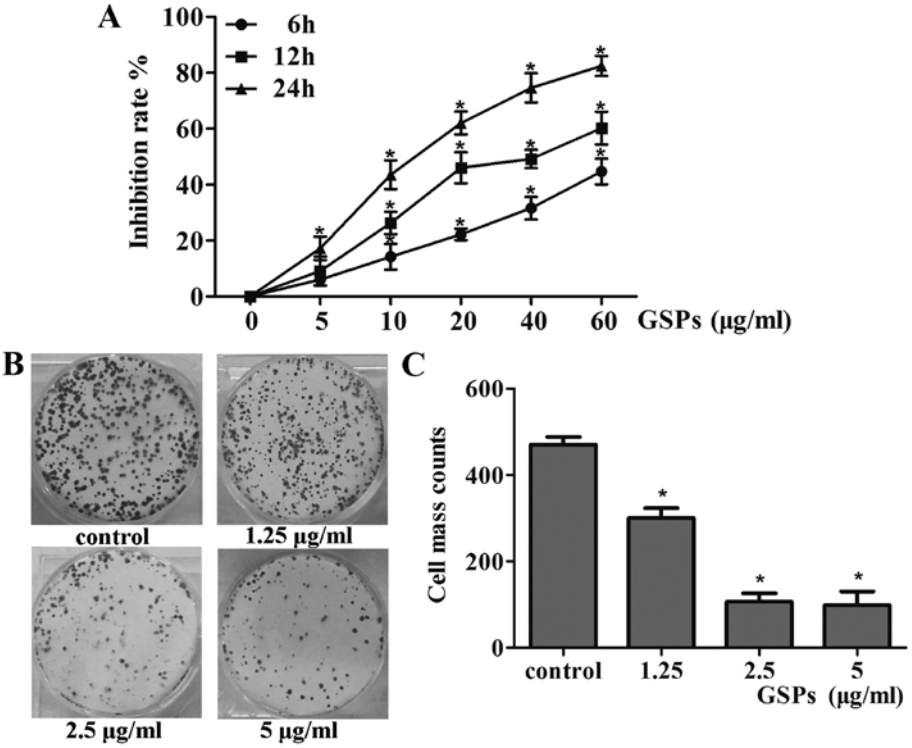

Figure 1. Antiproliferative activation of GSPs in CNE-2 cells. (A) CNE-2 cells were treated with varying doses of GSPs, and the relative viability of the cells was measured using the CCK-8 assay at 6, 12 and 24 h. (B) Cells (500) were seeded on 6-well plates and were treated with 1.25, 2.5 and 5 μg/ml GSPs or control for 10 days of culture. (C) The colony forming ability was measured by counting the colony number. Values are expressed as the mean ± SD of three experiments; $^{*}p<0.05$ vs. the control (non-GSP-treated).

Briefly, the cells were subjected to treatment with GSPs for 12 h, after which JC-1 staining solution was added to the plates and incubated at 37˚C for 20 min. JC-1 can then gather in the matrix of normal mitochondria as J-aggregates, emitting red fluorescence, but cannot accumulate in mitochondria with lower MMP and in that situation the JC-1 remains in a monomeric form, emitting green fluorescence. The collapse of the MMP is reflected by the color change of the dye from red to green, as analyzed by flow cytometry, in this case a FACSCanto II equipped with CellQuest software.

Protein extraction and western blot analysis. CNE-2 cells treated for 24 h with or without GSPs at the indicated concentrations were harvested and washed with ice-cold PBS, and then lysed on ice for 30 min using RIPA buffer supplemented with 20 mM Tris (pH 7.5), 1% Triton X-100, 150 mM NaCl and 1% of two types of protein inhibitors; phenylmethanesulfonyl fluoride (PMSF) and protein phosphatase inhibitor. Cellular extracts were clarified by centrifugation (Eppendorf, Hamburg, Germany) at 15,294 x g at 4˚C for 15 min, and protein concentrations were determined using the BCA assay (Beyotime Institute of Biotechnology). The extracted proteins were then subjected to western blot analysis, resolved on 10% Tris-glycine gels and transferred onto a polyvinylidene fluoride (PVDF) membrane (Immobilon-P; Millipore, Billerica, MA, USA). After blocking the non-specific binding sites with 5% skim milk for 1 h, the membranes were incubated overnight at 4˚C with specific primary antibodies. The membranes were incubated with the appropriate horseradish peroxidase-conjugated secondary antibody and then immunoreactive protein membranes were visualized using enhanced chemiluminescence (ECL). The protein bands were analyzed using a ChemiDoc XRS transilluminator (Bio-Rad). All blots shown are representative of three independent experiments.

Statistical analysis. All quantitative data are presented as mean ± SD of triplicate independent experiments. The statistical analyses were performed by one-way analysis of variance (ANOVA) using SPSS v.17.0 software. A p-value <0.05 was considered to indicate a statistically significant result.

Results

GSPs suppress the proliferation of NPC CNE-2 cells. GSPs significantly inhibited the survival of CNE-2 cells in a dose-dependent manner, with ranges observed from 6 to 44% following 6 h of exposure, 9-60% after 12 h, and 17-82% after 24 h ($p<0.05$), as shown in Fig. 1A. The observed effect also exhibited a time-dependent manner ($p<0.05$). Additionally, the half maximal inhibitory concentration (IC_{50} value) of GSPs in CNE-2 cells was 80.19 μg/ml at 6 h, 34.78 μg/ml at 12 h, and 14.48 μg/ml at 24 h. Based on these results, most subsequent experiments were carried out at 10, 20 and 40 μg/ml for 12 h. Further confirmation of the growth-suppressive property of GSPs was obtained using the colony formation assay, the results of which indicated that GSPs could reduce the colony forming efficiency of CNE-2 cells by 76.5, 38.66 and 19.16% after pre-treatment with 1.25, 2.5 and 5 μg/ml GSPs, respectively ($p<0.05$) (Fig. 1B and C). In combination, these results confirmed the inhibitory effects of GSPs in NPC cells.

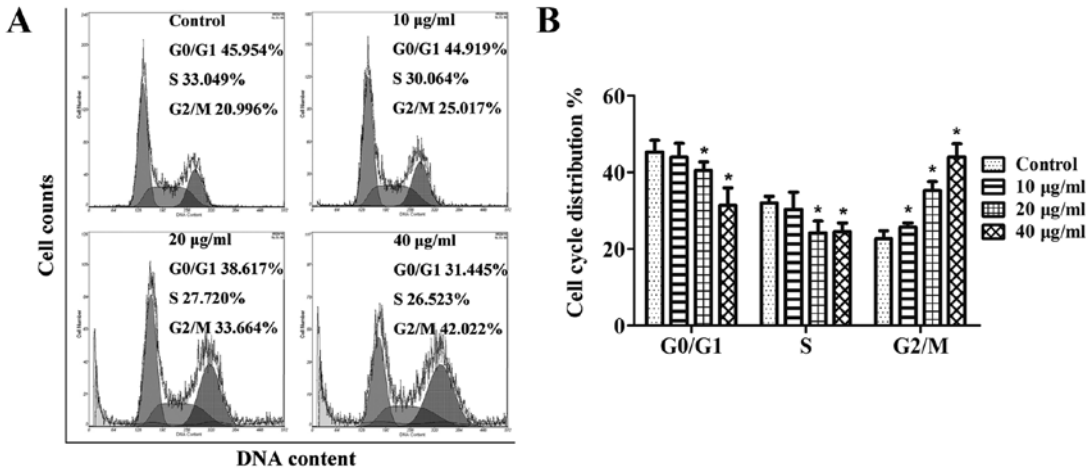

Figure 2. GSPs induce cell cycle arrest in the G2/M phase. (A) The representative cell cycle histograms of CNE-2 cells. (B) The treatment of CNE-2 cells with GSPs led to the accumulation of cells in the G2/M phase. Results are expressed as mean ± SD; *p<0.05 vs. the control.

GSPs induce G2/M phase cell cycle arrest in CNE-2 cells. Based on the significant inhibitory effect GSPs exerted on the growth of CNE-2 cells, we next aimed to determine whether the possible mechanism was related to the effect that GSPs had on the cell cycle progression of the CNE-2 cells. The results in Fig. 2A indicated that in NPC cells treated with GSPs, there was an obvious increase in the percentage of cells in G2/M phase at all the concentrations tested; 10 μg/ml (25%, p<0.05), 20 μg/ml (33.6%, p<0.05) and 40 μg/ml (42%, p<0.05) when compared to the control (non-GSP-treated) group (20.9%). Summarized in Fig. 2B are the results of cell cycle distribution analysis for each tested dose of the GSPs, which suggest that the inhibitory effect of the GSPs on the proliferation of CNE-2 cells may be associated with induction of G2/M phase arrest.

GSPs induce apoptosis of NPC CNE-2 cells. To determine the underlying mechanisms by which GSPs act to reduce NPC cell survival, we next investigated the morphological changes observed in cell nuclei induced by GSPs with Hoechst 333258 staining. CNE-2 cells treated with varying concentrations of GSPs for 12 h displayed classic changes, including chromatin agglutination, karyopyknosis and apoptotic body formation (Fig. 3A). Contrastingly, cells in the untreated control group displayed characteristics of almost normal cells, suggesting that GSPs induced the apoptosis of the NPC cells.

In order to provide further evidence that GSPs do induce apoptosis, quantitative analysis of apoptosis in the CNE-2 cells was analyzed by flow cytometry. Following a 12-h treatment with various doses of GSPs, the cells were stained with Annexin V-FITC/PI double dye and then typed as either early-stage (Annexin V^+ and PI^-) or late-stage apoptotic (Annexin V^+ and PI^+), as respectively shown in the E3 and E4 quadrants of the FACS histograms in Fig. 3B. The percentage of the total apoptotic population (including early- and late-stage) of the CNE-2 cells are further summarized in Fig. 3C, and were as follows: 2.1% in control cells (early-stage, 0.4% and late-stage, 1.7%), 18.7% in cells treated with 10 μg/ml GSPs (early-stage, 1.3% and late-stage, 17.4%; p<0.05), 36% in cells treated with 20 μg/ml GSPs (early-stage, 3.3% and late-stage, 32.7%, p<0.05), and 69.6% in cells treated with 40 μg/ml GSPs (early-stage, 7.1% and late-stage, 62.5%; p<0.05). Together, these results demonstrated that GSPs induced a significant increase in NPC CNE-2 cell apoptosis, both at the early and late stage (p<0.05).

GSPs induce disruption of MMP in CNE-2 cells. The depletion of mitochondrial transmembrane potential (MMP) ($\Delta\psi$m) is a hallmark of cellular apoptosis, linked to the initiation and activation of the apoptotic process in cells (10). Staining with the cationic lipophilic dye JC-1 was used to investigate the integrity of the mitochondrial membrane of the cells, so that the effect of GSPs on the MMP in CNE-2 cells could be determined. As shown in Fig. 4A, the staining resulted in a significant increase in green fluorescence-positive cells; 3.6% of the control group, 16.6% of the 10 μg/ml group, 38.4% of the 20 μg/ml group, and 58.0% of the 40 μg/ml group. The data revealed that treatment of CNE-2 cells with different concentrations of GSPs resulted in a dose-dependent increase in MMP levels (p<0.05) (Fig. 4B). Thus, we concluded that it was possible that the apoptotic effect observed in CNE-2 cells following GSP treatment is connected with the mitochondrial pathway and warrants further study.

GSPs activate caspase-3 and poly(ADP-ribose) polymerase (PARP). The release of apoptotic factors into the cytosol leads to the cleavage of caspase-3, which then cleaves various target proteins, including PARP, ultimately resulting in apoptotic cell death (24). As shown in Fig. 4C, data from the western blot analysis revealed a reduction in the levels of pro-caspase-3 and total PARP with a concomitant increase in the levels of cleaved caspase-3 and PARP (p<0.05). The relative expression levels of these proteins were also calculated through normalization to β-actin (Fig. 4D). These results indicated that the apoptosis of CNE-2 cells induced by GSPs may involve the activation of the caspase-3 pathway.

GSPs affect the protein expression of the Bcl-2 family. To assess whether or not treatment with GSPs induced cell death

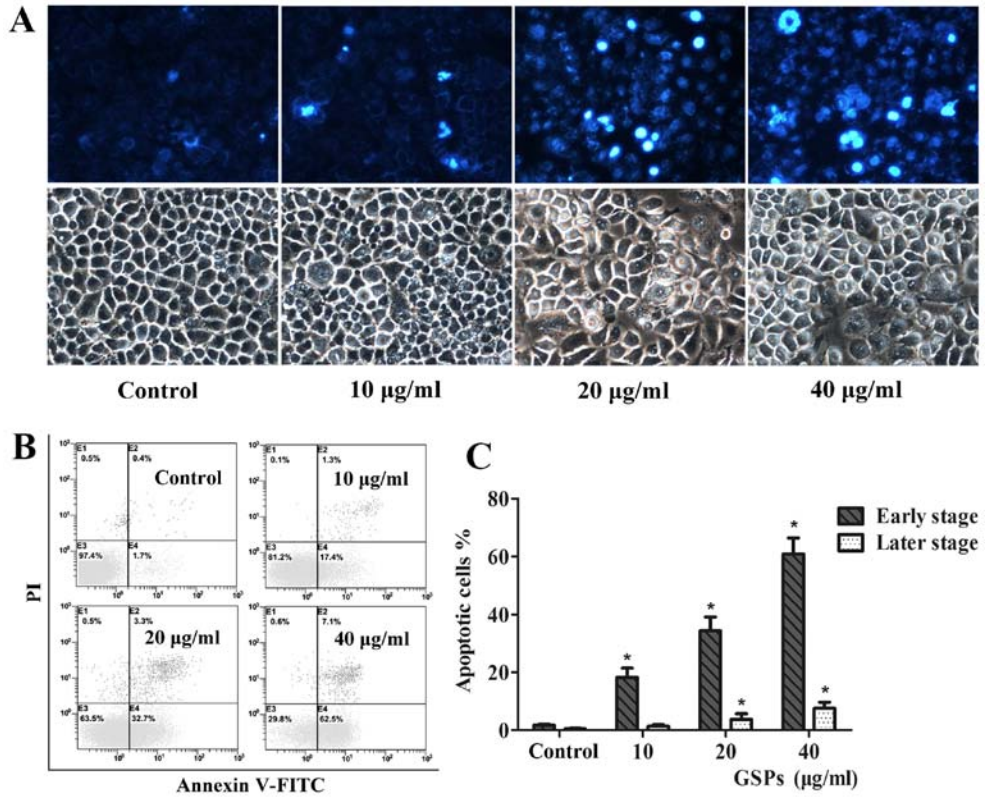

Figure 3. GSPs induce apoptosis of CNE-2 cells. (A) Morphological changes in nuclei were examined by fluorescence microscopy using Hoechst 33258 staining (magnification, x200). (B) Flow cytometric analysis of the Annexin V-FITC/PI double-stained CNE-2 cells. The E4 quadrant of the histograms indicates early-stage apoptotic cells, and the E2 quadrant indicates late-stage apoptotic cells. (C) The treatment of CNE-2 cells with GSPs resulted in significant increases in the percentages of apoptotic cells (including early- and late-stage). Values are expressed as the mean ± SD of three experiments; *p<0.05 vs. the control.

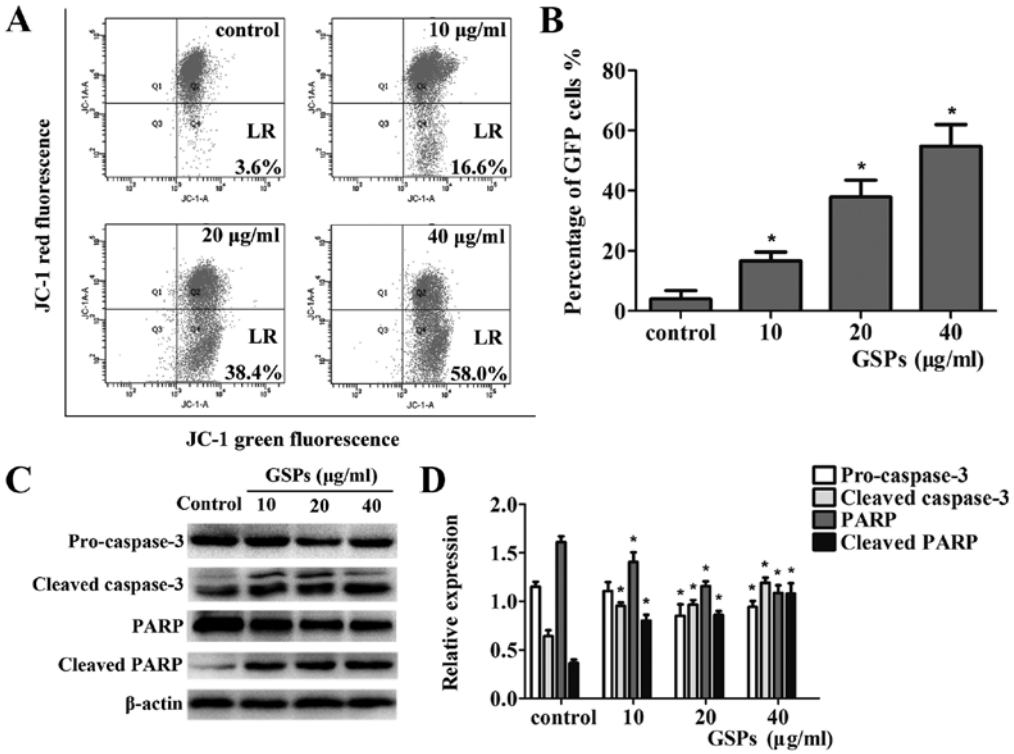

Figure 4. GSP-induced apoptosis in CNE-2 cells is mediated by the mitochondrial pathway. (A) The lower right (LR) quadrant of the histograms indicates the percentage of green fluorescence-positive (GFP) cells. (B) Treatment with GSPs resulted in a significant decrease in mitochondrial membrane potential in the CNE-2 cells. (C) Treatment of the CNE-2 cells with GSPs reduced the levels of pro-caspase-3 and PARP while GSP treatment increased the expression of cleaved caspase-3 and PARP in the cells. (D) The relative expression levels of the above proteins in the CNE-2 cells are summarized in a bar graph. Data are representative of three independent experiments and values are expressed as the mean ± SD; *p<0.05 vs. the control.

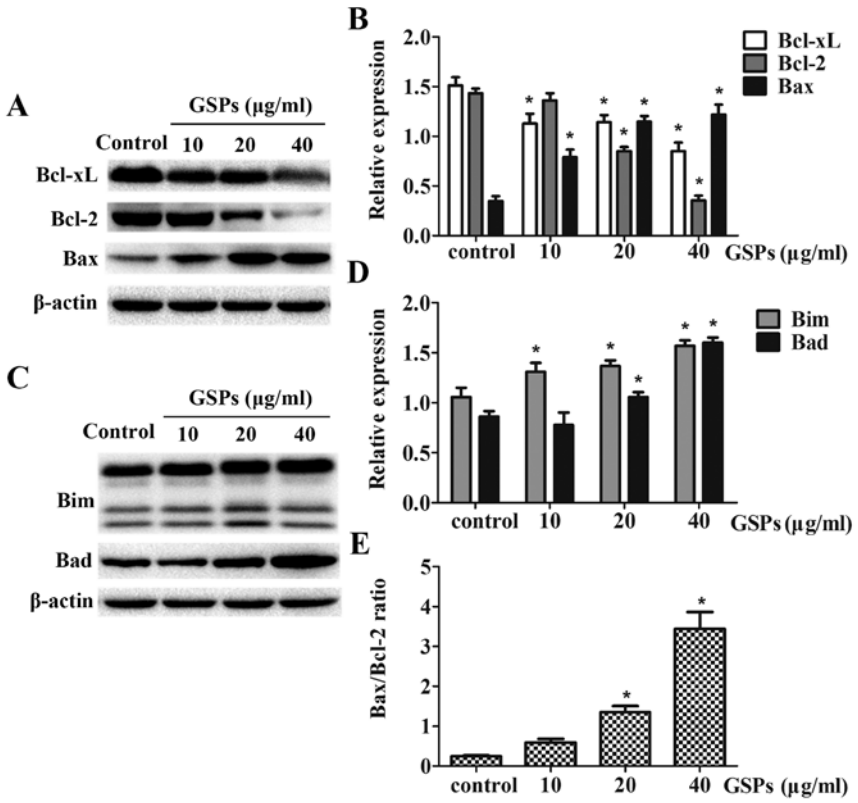

Figure 5. Expression of Bcl-2 family proteins in the CNE-2 cells following treatment with GSPs. (A) Treatment of CNE-2 cells with GSPs decreased the expression levels of anti-apoptotic proteins (Bcl-2 and Bcl-xL) while increasing pro-apoptotic protein Bax. (C) After treatment the expression of BH3-only proteins, Bim and Bad were reduced as determined by western blotting. (B and D) β-actin was used to verify equal loading of the protein samples and the relative of expression levels of the above proteins in the CNE-2 cells are summarized in a bar graph. (E) The ratio of Bax/Bcl-2 was markedly increased in a dose-dependent manner. Data are representative of three separate experiments with identical observations. Values are expressed as the mean ± SD; $^{*}p<0.05$ vs. the control.

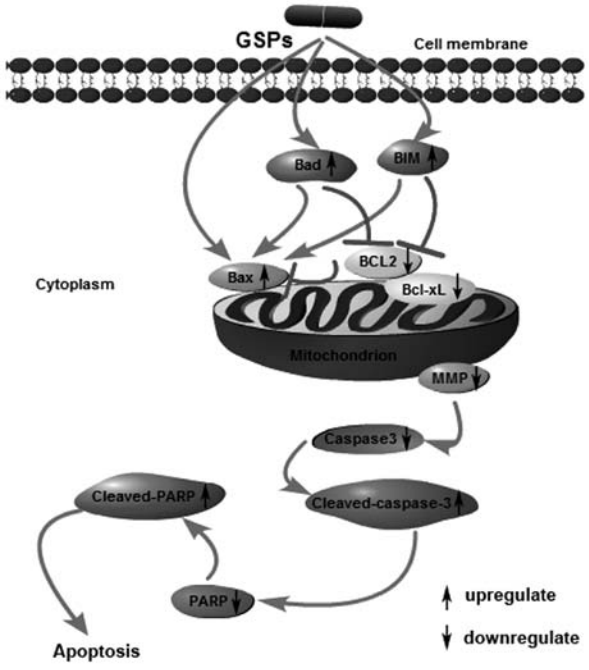

Figure 6. Mechanism of GSP-induced apoptosis in the NPC CNE-2 cells. GSPs upregulated the expression of Bax, Bim and Bad while downregulated the expression of Bcl-2 and Bcl-xL proteins. The loss of mitochondrial membrane potential (MMP) revealed that the integrity of the mitochondrial membrane was destroyed. Subsequently, the release of intermembrane space proteins activated caspase-3, which cleaved poly(ADP-ribose) polymerase (PARP) followed by cell apoptosis.

in NPC cells by affecting key regulators of apoptosis within the mitochondrial pathway, the expression of the proteins, Bax, Bcl-2, Bcl-xL, Bim and Bad was examined using western blot analysis. Treatment of CNE-2 cells with GSPs for 12 h resulted in a dose-dependent reduction in protein expression of Bcl-2 and Bcl-xL, whereas the expression levels of Bax, Bim and Bad were upregulated with increasing concentrations of GSPs (Fig. 5). GSP treatment also resulted in an obvious increase in the ratio of Bax/Bcl-2, which is crucial in determining the survival or death of cells following an apoptotic stimulus (Fig. 5E). The relative expression levels of these proteins were calculated by normalization to β-actin expression, and were analyzed by Image gray analysis software, which revealed a dose-dependent trend.

Discussion

Interest in the biology of grape seed extract first originated with reports that moderate red wine consumption may be associated with a low incidence of coronary heart disease, as observed in the population of France. More recently, GSPs have been extensively studied for their potential anticancer or chemopreventative properties. Dhanalakshmi *et al* observed that GSPs could inhibit the nuclear factor-κB (NF-κB) pathway and induce the apoptosis of DU145 prostate carcinoma cells (19). It has also been found that dietary intake of GSPs was effective in inhibiting the development of UV-induced

skin tumors in SKH-1 hairless mice, which was associated with the inhibition of oxidative stress and inflammatory responses (20). Furthermore, it has been demonstrated that GSPs exert anticancer effects against cervical cancer through the mitochondrial apoptosis pathway (16). However, a nasopharyngeal carcinoma (NPC)-specific effect or mechanism of GSPs have not yet been seen. In the present study, we first found that GSPs could attenuate the viability of CNE-2 cells in a dose- and time-dependent manner, leading to significant cell cycle arrest at the G2/M phase (Figs. 1 and 2). This suggested that blocking cell cycle progression could be an effective strategy to halt the development of NPC.

It has been reported that apoptosis can effectively prevent cancer development through the culling of cells that are at risk of transformation, and that evasion of apoptosis is a characteristic present in numerous cancers that exhibit therapeutic resistance (21). Thus, it can be reasonably argued that the best treatment for cancer is to induce cellular apoptosis. In the present study, our findings revealed that GSPs could notably induce apoptosis in CNE-2 cells accompanied by morphological changes in the cell nuclei (Fig. 3). In the presence of oncogenic stress, the mitochondrial pathway is triggered and the activity of the anti-apoptotic Bcl-2 proteins is suppressed, followed by the oligomerization of Bak and Bax proteins to induce MOMP (11). The present study has shown that CNE-2 cells expressed significantly less Bcl-2 and Bcl-xL proteins, but more Bax protein, suggesting that the Bax/Bcl-2 ratio was markedly increased in GSP-induced apoptosis (Fig. 5A and E). Furthermore, GSPs depleted the mitochondrial membrane potential (MMP) to a very low level (Fig. 4A). Importantly, the activation of Bax and Bak requires direct interaction with several BH3-only proteins, while the other BH3-only proteins promote death indirectly by neutralizing the activity of anti-apoptotic Bcl-2 proteins (22). Our results also indicated that exposure to GSPs increased the expression levels of the BH3-only proteins Bim and Bad in CNE-2 cells (Fig. 5C). Moreover, proteins in the intermembrane space responsible for the activation of caspases were released following MOMP. Cleaved caspase-3 can then go on to cleave hundreds of different substrates in parallel, including PARP, all within minutes, leading to rapid cell death with the characteristic morphological hallmarks (23). Our data demonstrated that GSPs decreased the expression of pro-caspase-3 and PARP, whereas the levels of cleaved-caspase-3 and cleaved-PARP were increased (Fig. 4C). When considered together, these findings lend support to our hypothesis that, in NPC CNE-2 cells, GSPs induced apoptosis via the mitochondrial pathway.

Upon consideration of our results as well as other previous research, we speculated that GSPs could induce the apoptosis of human NPC CNE-2 cells through the mitochondrial pathway, characterized by stimulating cell membrane receptors to upregulate the expression of Bax, Bim and Bad, while downregulating the expression of Bcl-2 and Bcl-xL, as shown in Fig. 6. The loss of MMP revealed that the integrity of the mitochondrial membrane was destroyed. Subsequently, the release of proteins in the intermembrane space activated caspase-3, which cleaved poly(ADP-ribose) polymerase (PRAP), resulting in cell apoptosis. Thus, GSPs appear to be plausible candidates as a bioactive phytochemical effective for the treatment of NPC. In summation, the results of the present study have demonstrated the chemotherapeutic potential of GSPs based on their effects on the induction of apoptosis in NPC CNE-2 cells. However, the specific components of GSPs responsible for this induction of apoptosis still need to be identified, and our future aims are focused on this goal as well as determining whether GSPs also exert an inhibitory effect *in vivo*.

Acknowledgements

The present study was financially supported by grants from the National Natural Science Foundation of China (no. 81272434), the Traditional Chineses Medicine Bureau of Guangdong Province (no. 2014154), and the Cultivation Foundation of Guangdong Medical University (M2014003).

References

1. Chua ML, Wee JT, Hui EP and Chan AT: Nasopharyngeal carcinoma. Lancet 387: 1012-1024, 2016.
2. Lee AW, Sze WM, Au JS, Leung SF, Leung TW, Chua DT, Zee BC, Law SC, Teo PM, Tung SY, *et al*: Treatment results for nasopharyngeal carcinoma in the modern era: The Hong Kong experience. Int J Radiat Oncol Biol Phys 61: 1107-1116, 2005.
3. Lee AW, Ng WT, Chan LL, Hung WM, Chan CC, Sze HC, Chan OS, Chang AT and Yeung RM: Evolution of treatment for nasopharyngeal cancer - success and setback in the intensity-modulated radiotherapy era. Radiother Oncol 110: 377-384, 2014.
4. Lin S, Pan J, Han L, Guo Q, Hu C, Zong J, Zhang X and Lu JJ: Update report of nasopharyngeal carcinoma treated with reduced-volume intensity-modulated radiation therapy and hypothesis of the optimal margin. Radiother Oncol 110: 385-389, 2014.
5. Yi J, Huang X, Gao L, Luo J, Zhang S, Wang K, Qu Y, Xiao J and Xu G: Intensity-modulated radiotherapy with simultaneous integrated boost for locoregionally advanced nasopharyngeal carcinoma. Radiat Oncol 9: 56, 2014.
6. Zheng Y, Han F, Xiao W, Xiang Y, Lu L, Deng X, Cui N and Zhao C: Analysis of late toxicity in nasopharyngeal carcinoma patients treated with intensity modulated radiation therapy. Radiat Oncol 10: 17, 2015.
7. Wei Z, Xie Y, Xu J, Luo Y, Chen F, Yang Y, Huang Q, Tang A and Huang G: Radiation-induced sarcoma of head and neck: 50 years of experience at a single institution in an endemic area of nasopharyngeal carcinoma in China. Med Oncol 29: 670-676, 2012.
8. Strasser A, Cory S and Adams JM: Deciphering the rules of programmed cell death to improve therapy of cancer and other diseases. EMBO J 30: 3667-3683, 2011.
9. Lopez J and Tait SW: Mitochondrial apoptosis: Killing cancer using the enemy within. Br J Cancer 112: 957-962, 2015.
10. Westphal D, Dewson G, Czabotar PE and Kluck RM: Molecular biology of Bax and Bak activation and action. Biochim Biophys Acta 1813: 521-531, 2011.
11. Hockenbery D, Nuñez G, Milliman C, Schreiber RD and Korsmeyer SJ: Bcl-2 is an inner mitochondrial membrane protein that blocks programmed cell death. Nature 348: 334-336, 1990.
12. Kurahashi N, Inoue M, Iwasaki M, Tanaka Y, Mizokami M and Tsugane S; JPHC Study Group: Vegetable, fruit and antioxidant nutrient consumption and subsequent risk of hepatocellular carcinoma: A prospective cohort study in Japan. Br J Cancer 100: 181-184, 2009.
13. Katiyar SK and Athar M: Grape seeds: Ripe for cancer chemoprevention. Cancer Prev Res 6: 617-621, 2013.
14. Prasad R, Vaid M and Katiyar SK: Grape proanthocyanidin inhibit pancreatic cancer cell growth in vitro and in vivo through induction of apoptosis and by targeting the PI3K/Akt pathway. PLoS One 7: e43064, 2012.
15. Derry MM, Raina K, Balaiya V, Jain AK, Shrotriya S, Huber KM, Serkova NJ, Agarwal R and Agarwal C: Grape seed extract efficacy against azoxymethane-induced colon tumorigenesis in A/J mice: Interlinking miRNA with cytokine signaling and inflammation. Cancer Prev Res 6: 625-633, 2013.

16. Chen Q, Liu XF and Zheng PS: Grape seed proanthocyanidins (GSPs) inhibit the growth of cervical cancer by inducing apoptosis mediated by the mitochondrial pathway. PLoS One 9: e107045, 2014.
17. Singh T, Sharma SD and Katiyar SK: Grape proanthocyanidins induce apoptosis by loss of mitochondrial membrane potential of human non-small cell lung cancer cells in vitro and in vivo. PLoS One 6: e27444, 2011.
18. Nandakumar V, Singh T and Katiyar SK: Multi-targeted prevention and therapy of cancer by proanthocyanidins. Cancer Lett 269: 378-387, 2008.
19. Dhanalakshmi S, Agarwal R and Agarwal C: Inhibition of NF-kappaB pathway in grape seed extract-induced apoptotic death of human prostate carcinoma DU145 cells. Int J Oncol 23: 721-727, 2003.
20. Sharma SD, Meeran SM and Katiyar SK: Dietary grape seed proanthocyanidins inhibit UVB-induced oxidative stress and activation of mitogen-activated protein kinases and nuclear factor-kappaB signaling in in vivo SKH-1 hairless mice. Mol Cancer Ther 6: 995-1005, 2007.
21. Kelly GL and Strasser A: The essential role of evasion from cell death in cancer. Adv Cancer Res 111: 39-96, 2011.
22. Ku B, Liang C, Jung JU and Oh BH: Evidence that inhibition of BAX activation by BCL-2 involves its tight and preferential interaction with the BH3 domain of BAX. Cell Res 21: 627-641, 2011.
23. Park D and Dilda PJ: Mitochondria as targets in angiogenesis inhibition. Mol Aspects Med 31: 113-131, 2010.